Role of Surface Termination and Quantum Size in α-$CsPbX_3$ (X = Cl, Br, I) 2D Nanostructures for Solar Light Harvesting

Giovanni Di Liberto,[1] Ornella Fatale,[1,2] and Gianfranco Pacchioni[1]*

1) Dipartimento di Scienza dei Materiali, Università di Milano - Bicocca, via R. Cozzi 55, 20125 Milano, Italy
2) Università di Pisa, Dipartimento di Chimica e Chimica Industriale, via G. Moruzzi 13, 56124 Pisa, Italy

Electronic Supporting Information

S1 Bulk $CsPbX_3$ effective masses

The reduced effective mass (m*) of $CsPbCl_3$, $CsPbBr_3$, and $CsPbI_3$ has been evaluated at fully optimized bulk structure from the curvature of the band structure.[1] In particular, we first evaluated electron's (m_e*) and hole's (m_h*) effective mass, then m* was calculated as $\frac{1}{m^*} = \frac{1}{m_e^*} + \frac{1}{m_h^*}$.

Table S1*:* Calculated reduced effective mass of $CsPbCl_3$, $CsPbBr_3$, and $CsPbI_3$. Values are given in electron mass units (m_0).

	$CsPbCl_3$	$CsPbBr_3$	$CsPbI_3$
m*, this work	0.12	0.07	0.06
m*, Ref [2]	0.09	0.07	0.06
m*, exp.[3]	/	/	0.12

S2 Structural and Electronic properties of $CsPbCl_3$ (001) and (110) surfaces

Table S2: Calculated slab thickness (d), lattice parameter (a), lattice angle (β), band gap (E_g), surface energy (γ), Valence Band Maximum (VBM) of $CsPbCl_3$ (001) slab models $PbCl_2$ and CsCl-terminated. Results are obtained with HSE06 functional.

$PbCl_2$-terminated surface							
Layers	Atoms	d / nm	a / Å	β / °	E_g / eV	γ / Jm^{-2}	VBM / eV
3	8	0.5	5.599	90	3.94	0.20	-5.38

5	13	1.1	5.617	90	3.58	0.17	-4.93
7	18	1.6	5.622	90	3.50	0.16	-4.84
9	23	2.2	5.626	90	3.39	0.16	-4.72
11	28	2.8	5.629	90	3.30	0.16	-4.63
13	33	3.3	5.631	90	3.23	0.16	-4.57
15	38	3.9	5.633	90	3.18	0.16	-4.52
17	43	4.5	5.634	90	3.14	0.16	-4.49
19	48	5.0	5.635	90	3.12	0.16	-4.47
CsCl-terminated surface							
Layers	Atoms	d / nm	a / Å	β / °	E_g / eV	γ / Jm^{-2}	*VBM* / eV
3	7	0.5	5.583	90	3.53	0.19	-3.92
5	12	1.1	5.627	90	3.36	0.17	-3.95
7	17	1.6	5.636	90	3.25	0.16	-3.87
9	22	2.2	5.639	90	3.18	0.16	-3.81
11	27	2.8	5.640	90	3.14	0.16	-3.76
13	32	3.3	5.641	90	3.11	0.16	-3.74
15	37	3.9	5.641	90	3.09	0.16	-3.72
17	42	4.5	5.642	90	3.08	0.16	-3.70
19	47	5.0	5.642	90	3.07	0.16	-3.69

Table S3: Calculated slab thickness (d), lattice parameters (a, b), lattice angle (β), band gap (E_g), surface energy (γ), Valence Band Maximum (*VBM*) of $CsPbCl_3$ (110) slab models Cl, Cs, and PbCl-terminated. Results are obtained with HSE06 functional.

Cl-terminated surface								
Layers	Atoms	d / nm	a / Å	b / Å	β / °	E_g / eV	γ / Jm^{-2}	*VBM* / eV
5	10	0.7	5.692	7.390	90	4.51	0.21	-6.25
7	15	1.1	5.654	7.601	90	4.08	0.22	-5.88
9	20	1.5	5.688	7.608	90	3.83	0.20	-5.70
11	25	1.9	5.663	7.512	90	3.60	0.21	-5.42
13	30	2.3	5.700	7.674	90	3.54	0.19	-5.43
15	35	2.7	5.685	7.640	90	3.50	0.19	-5.43
17	40	3.0	5.702	7.769	90	3.38	0.17	-5.24
19	45	3.5	5.690	7.735	90	3.36	0.17	-5.22
21	50	3.8	5.708	7.742	90	3.35	0.14	-5.24
Cs-terminated surface								
Layers	Atoms	d / nm	a / Å	b / Å	β / °	E_g / eV	γ / Jm^{-2}	*VBM* / eV
5	9	0.7	5.528	7.614	90	4.16	0.34	-2.62
7	14	1.1	5.599	7.687	90	3.90	0.28	-2.92

9	19	1.5	5.621	7.763	90	3.61	0.27	-2.82
11	24	1.9	5.628	7.813	90	3.44	0.27	-2.70
13	29	2.3	5.631	7.849	90	3.32	0.27	-2.62
15	34	2.7	5.633	7.872	90	3.25	0.27	-2.57
17	39	3.1	5.635	7.890	90	3.20	0.27	-2.54
19	44	3.5	5.636	7.902	90	3.17	0.27	-2.52
21	49	3.9	5.637	7.910	90	3.14	0.27	-2.49
PbCl-terminated surface								
Layers	Atoms	*d* / nm	*a* / Å	*b* / Å	*β* / °	E_g / eV	*γ* / Jm^{-2}	*VBM* / eV
5	11	0.8	5.608	8.052	90	3.84	0.60	-5.17
7	16	1.1	5.607	8.090	90	3.97	0.55	-5.15
9	21	1.5	5.613	8.100	90	3.77	0.54	-4.88
11	26	1.9	5.615	8.097	90	3.60	0.54	-4.67
13	31	2.3	5.620	8.089	90	3.46	0.53	-4.53
15	36	2.7	5.623	8.082	90	3.36	0.53	-4.41
17	41	3.1	5.625	8.072	90	3.28	0.53	-4.33
19	46	3.5	5.627	8.066	90	3.22	0.53	-4.27
21	51	3.9	5.629	8.060	90	3.18	0.53	-4.22

S3 Structural and Electronic properties of $CsPbBr_3$ (001) and (110) surfaces

Table S4: Calculated slab thickness (*d*), lattice parameter (*a*), lattice angle (*β*), band gap (E_g), surface energy (γ), Valence Band Maximum (*VBM*) of $CsPbBr_3$ (001) slab models $PbBr_2$ and CsBr-terminated. Results are obtained with HSE06 functional.

$PbBr_2$-terminated surface							
Layers	Atoms	*d* / nm	*a* / Å	*β* / °	E_g / eV	*γ* / Jm^{-2}	*VBM* / eV
3	8	0.5	5.848	90	3.24	0.18	-5.41
5	13	1.1	5.871	90	3.00	0.16	-5.17
7	18	1.7	5.876	90	2.89	0.15	-5.10
9	23	2.3	5.881	90	2.77	0.15	-5.03
11	28	2.9	5.883	90	2.68	0.15	-4.97
13	33	3.5	5.886	90	2.62	0.15	-4.93
15	38	4.1	5.887	90	2.57	0.15	-4.90
17	43	4.7	5.888	90	2.54	0.15	-4.87
19	48	5.2	5.889	90	2.52	0.15	-4.86
CsBr-terminated surface							
Layers	Atoms	*d* / nm	*a* / Å	*β* / °	E_g / eV	*γ* / Jm^{-2}	*VBM* / eV
3	7	0.6	5.835	90	2.94	0.16	-4.15
5	12	1.1	5.876	90	2.79	0.14	-4.14
7	17	1.7	5.885	90	2.66	0.13	-4.01

9	22	2.3	5.889	90	2.56	0.13	-3.92
11	27	2.9	5.890	90	2.52	0.13	-3.86
13	32	3.5	5.892	90	2.49	0.13	-3.82
15	37	4.1	5.893	90	2.46	0.13	-3.79
17	42	4.7	5.893	90	2.44	0.13	-3.77
19	47	5.3	5.896	90	2.43	0.13	-3.75

Table S5: Calculated slab thickness (*d*), lattice parameters (*a, b*), lattice angle (β), band gap (E_g), surface energy (γ), Valence Band Maximum (*VBM*) of $CsPbBr_3$ (110) slab models Br, Cs, and PbBr-terminated. Results are obtained with HSE06 functional.

Br-terminated surface								
Layers	Atoms	*d* / nm	*a* / Å	*b* / Å	β / °	E_g / eV	γ / Jm^{-2}	*VBM* / eV
5	10	0.7	5.929	7.809	90	3.77	0.18	-6.18
7	15	1.1	5.900	8.008	90	3.38	0.20	-5.93
9	20	1.5	5.923	8.102	90	3.13	0.20	-5.72
11	25	2.0	5.907	8.168	90	2.93	0.21	-5.53
13	30	2.4	5.930	8.172	90	2.86	0.20	-5.47
15	35	2.8	5.917	8.192	90	2.76	0.20	-5.38
17	40	3.2	5.934	8.201	90	2.74	0.19	-5.35
19	45	3.6	5.923	8.208	90	2.68	0.20	-5.31
21	50	4.0	5.935	8.217	90	2.68	0.19	-5.30
Cs-terminated surface								
Layers	Atoms	*d* / nm	*a* / Å	*b*/ Å	β / °	E_g / eV	γ / Jm^{-2}	*VBM* / eV
5	9	0.7	5.779	8.154	90	3.55	0.30	-2.83
7	14	1.1	5.849	8.210	90	3.34	0.25	-3.08
9	19	1.5	5.874	8.271	90	3.05	0.23	-2.96
11	24	1.9	5.881	8.297	90	2.87	0.23	-2.85
13	29	2.3	5.884	8.312	90	2.75	0.23	-2.76
15	34	2.8	5.886	8.320	90	2.68	0.23	-2.70
17	39	3.2	5.888	8.323	90	2.62	0.23	-2.65
19	44	3.6	5.889	8.325	90	2.58	0.23	-2.62
21	49	4.0	5.890	8.326	90	2.55	0.23	-2.60
PbBr-terminated surface								
Layers	Atoms	*d* / nm	*a* / Å	*b* / Å	β / °	E_g / eV	γ / Jm^{-2}	*VBM* / eV
5	11	0.8	5.853	8.364	90	3.09	0.51	-5.29
7	16	1.2	5.859	8.399	90	3.24	0.48	-5.31
9	21	1.6	5.865	8.403	90	3.14	0.47	-5.18
11	26	2.0	5.871	8.405	90	3.00	0.47	-5.03
13	31	2.4	5.873	8.401	90	2.88	0.47	-4.91
15	36	2.9	5.877	8.394	90	2.78	0.47	-4.82

17	41	3.3	5.879	8.387	90	2.71	0.47	-4.75
19	46	3.7	5.881	8.383	90	2.65	0.47	-4.70
21	51	4.1	5.882	8.380	90	2.61	0.47	-4.68

S4 Structural and Electronic properties of $CsPbI_3$ (001) and (110) surfaces

Table S6: Calculated slab thickness (*d*), lattice parameter (*a*), lattice angle (β), band gap (E_g), surface energy (γ), Valence Band Maximum (*VBM*) of $CsPbI_3$ (001) slab models PbI_2 and CsI-terminated. Results are obtained with HSE06 functional.

PbI_2-terminated surface							
Layers	Atoms	*d* / nm	*a* / Å	β / °	E_g / eV	γ / Jm^{-2}	*VBM* / eV
3	8	0.6	6.182	90	2.30	0.20	-5.03
5	13	1.2	6.192	90	2.28	0.19	-5.06
7	18	1.8	6.193	90	2.16	0.18	-5.03
9	23	2.4	6.192	90	2.06	0.18	-4.98
11	28	3.1	6.191	90	1.98	0.18	-4.94
13	33	3.7	6.190	90	1.93	0.18	-4.90
15	38	4.3	6.189	90	1.89	0.18	-4.87
17	43	4.9	6.189	90	1.86	0.18	-4.85
19	48	5.5	6.188	90	1.84	0.18	-4.83
CsI-terminated surface							
Layers	Atoms	*d* / nm	*a* / Å	β / °	E_g / eV	γ / Jm^{-2}	*VBM* / eV
3	7	0.6	6.123	90	2.25	0.15	-3.68
5	12	1.2	6.165	90	2.13	0.13	-3.66
7	17	1.8	6.176	90	2.00	0.12	-3.52
9	22	2.4	6.180	90	1.92	0.12	-3.43
11	27	3.1	6.181	90	1.86	0.12	-3.37
13	32	3.7	6.182	90	1.81	0.12	-3.31
15	37	4.3	6.182	90	1.78	0.12	-3.28
17	42	4.9	6.183	90	1.76	0.12	-3.26
19	47	5.5	6.183	90	1.74	0.12	-3.24

Table S7: Calculated slab thickness (*d*), lattice parameters (*a, b*), lattice angle (β), band gap (E_g), surface energy (γ), Valence Band Maximum (*VBM*) of $CsPbI_3$ (110) slab models I, Cs, and PbI-terminated. Results are obtained with HSE06 functional.

I-terminated surface								
Layers	Atoms	*d* / nm	*a* / Å	*b* / Å	β / °	E_g / eV	γ / Jm^{-2}	*VBM* / eV

5	10	0.8	6.225	8.334	90	2.91	0.18	-5.46
7	15	1.2	6.197	8.454	90	2.61	0.20	-5.35
9	20	1.6	6.242	8.560	90	2.39	0.19	-5.19
11	25	2.1	6.214	8.591	90	2.30	0.20	-5.08
13	30	2.5	6.250	8.586	90	2.18	0.18	-5.03
15	35	2.9	6.224	8.613	90	2.07	0.20	-4.96
17	40	3.4	6.253	8.600	90	2.08	0.18	-4.96
19	45	3.8	6.233	8.606	90	2.00	0.19	-4.92
21	50	4.2	6.251	8.618	90	2.02	0.17	-4.90
Cs-terminated surface								
Layers	Atoms	d / nm	a / Å	b / Å	β / °	E_g / eV	γ / Jm^{-2}	*VBM* / eV
5	9	0.7	6.059	8.489	90	2.80	0.28	-2.28
7	14	1.1	6.143	8.534	90	2.70	0.22	-2.62
9	19	1.6	6.165	8.601	90	2.46	0.37	-2.56
11	24	2.0	6.173	8.635	90	2.27	0.20	-2.44
13	29	2.4	6.176	8.660	90	2.14	0.20	-2.34
15	34	2.9	6.178	8.678	90	2.05	0.20	-2.26
17	39	3.3	6.179	8.689	90	1.98	0.20	-2.21
19	44	3.8	6.180	8.697	90	1.93	0.20	-2.17
21	49	4.2	6.181	8.703	90	1.90	0.20	-2.14
PbI-terminated surface								
Layers	Atoms	d / nm	a / Å	b / Å	β / °	E_g / eV	γ / Jm^{-2}	*VBM* / eV
5	11	0.9	6.121	8.849	90	2.19	0.51	-4.88
7	16	1.3	6.160	8.858	90	2.29	0.49	-4.90
9	21	1.7	6.170	8.828	90	2.23	0.32	-4.85
11	26	2.2	6.174	8.811	90	2.17	0.48	-4.78
13	31	2.6	6.177	8.798	90	2.10	0.48	-4.72
15	36	3.0	6.178	8.790	90	2.04	0.48	-4.67
17	41	3.5	6.179	8.784	90	1.99	0.48	-4.61
19	46	3.9	6.180	8.779	90	1.95	0.48	-4.58
21	51	4.3	6.181	8.776	90	1.92	0.48	-4.54

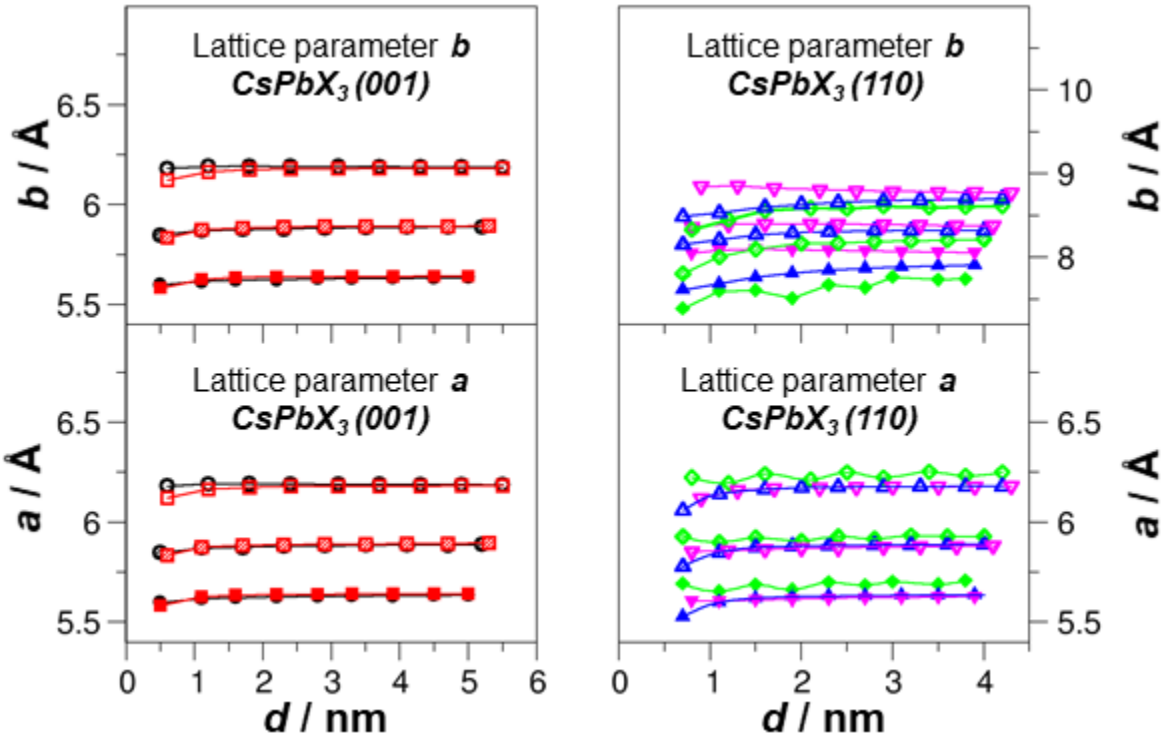

Figure S1: Lattice vectors *a* and *b* of the five $CsPbX_3$ (001) and (110) surface terminations as a function of the slab thickness. Black Circles: PbX_2-(001); red squares: CsX-(001); green diamonds: X-(110); blue triangles-up: Cs-(110); magenta triangles-down: PbX-(110). Solid shapes: $CsPbCl_3$, striped shapes: $CsPbBr_3$, empty shapes: $CsPbI_3$. (001) surface have a square lattice, *i.e.* $a = b$, (110) surface have a rectangular lattice.

S5 TiO_2 (101) surfaces

The computational setup has been kept unchanged from that used for $CsPbX_3$. The basis sets of Ti and O have been taken from the CRYSTAL database, and we chose the same family adopted for X atoms, i.e. TZVP basis set.[4] The HSE06 functional has been demonstrated to the a reliable an accurate choice for the treatment of oxides, including TiO_2.[5,6]

We started from the experimental crystal structure[7] of anatase TiO_2 and we fully optimized the bulk model. The optimized lattice vectors and band gap are reported in Table S5, and we see that both the structural and electronic properties are well reproduced.

Table S8: Calculated lattice vectors (*a* and *c*) and band gap (E_g) of bulk TiO_2.

Model	*a* / Å	*c* / Å	E_g / eV
DFT/HSE06	3.771	9.543	3.56
Exp	3.785[7]	9.514[7]	3.20-3.44[8,9]

We then started from the optimized bulk structure to design (101) slabs of increasing thickness, which is recognized as the most representative anatase surface.[10] We investigated slab models up to 2.5 nm thick. The calculated structural and electronic properties are reported in Table S8. We can see that TiO2 (101) properties converge with slab model 2 nm thick.

Table S9*:* Calculated slab thickness (*d*), lattice parameter (*a*), lattice angle (β), band gap (E_g), surface energy (γ), Valence Band Maximum (*VBM*) of TiO_2 (101) slab models. Results are obtained with HSE06 functional**.**

TiO_2 (101)								
Layers	Atoms	*d* / nm	*a* / Å	*b* / Å	β / °	E_g / eV	γ / Jm^{-2}	*VBM* / eV
6	12	0.3	3.527	10.359	90	4.67	0.48	-8.98
12	24	0.6	3.704	10.309	90	4.47	0.55	-8.63
18	36	0.9	3.723	10.284	90	4.05	0.60	-8.40
24	48	1.3	3.734	10.280	90	3.84	0.62	-8.30
30	60	1.6	3.741	10.276	90	3.73	0.64	-8.26
36	72	2.0	3.746	10.270	90	3.66	0.65	-8.24
42	84	2.3	3.749	10.269	90	3.63	0.66	-8.23
48	96	2.6	3.752	10.269	90	3.61	0.66	-8.23

S6 Band alignment in TiO_2/$CsPbX_3$ heterostructures

$CsPbX_3$ nanostructures are usually combined with oxides, such as anatase TiO_2, leading to heterojunctions with higher efficiency in solar light absorption and, at the same time, high capability to separate photogenerated charge carriers after light absorption. Usually, these materials display excellent photoelectrochemical properties due to efficient injection of electrons on TiO_2 nanostructures, and then to active redox species. For instance, it has been recently shown that combining $CsPbI_3$ with TiO_2 leads to almost 99% efficiency in electron injection from the perovskite to TiO_2.[11] At the same time, a $CsPbBr_3$/TiO_2 heterostructure has been successfully used for CO_2 photoreduction. [12]

A suitable positioning of the band edges for charge-carriers separation is that of type-II heterostructures, in which both *VBM* and *CBM* of one species are lower in energy than the other component. In the case of $CsPbX_3$/TiO_2 the requirement is to have *VBM* and *CBM* of $CsPbX_3$ higher in energy than the those of TiO_2, to promote the electron transfer from the perovskite to TiO_2 after visible light absorption.[11,12]

The thickness-converged band edges of $CsPbX_3$ X-(110) can be used to estimate the relative band edges positions in $CsPbX_3$/TiO_2 composites.[11,12] $CsPbX_3$ values are compared with thickness-converged TiO_2 data (see above). The comparison of the band edges positioning of the isolated units is a simple and reasonably reliable approach for the prediction of band alignment in a composite system, at least when no major reconstructions occur at the interface.[13–15] It must be mentioned, however, that the approach of using the band positions of the separate units neglects effects due to the formation of an explicit interface between the two moieties.

Figure S2 shows that the combination of $CsPbX_3$ with TiO_2 leads effectively to a type-II alignment. In particular, electrons should be promoted and injected into the TiO_2 conduction band. From the reported diagram, the highest band offset is expected for $CsPbI_3$, but all three perovskites considered

in this work exhibit a suitable band alignment. These results provide a rationalization for the observed properties in $CsPbX_3/TiO_2$ composites.[11,12]

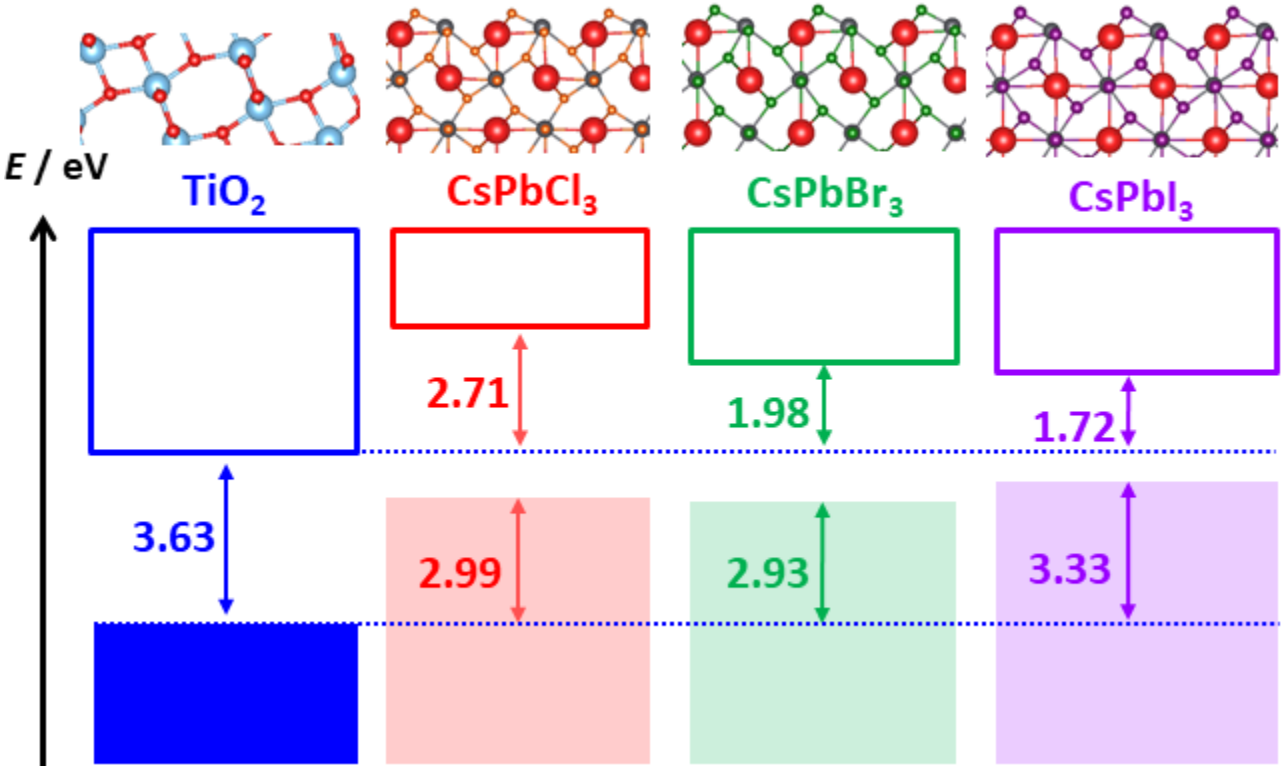

Figure S2: Band edges positioning of $CsPbX_3$ (110) and TiO_2 (101) moieties in $CsPbX_3/TiO_2$ heterojunctions (the data are for thickness-converged slab models at the DFT/HSE06 level).

S6 Benchmark on DFT/HSE06 and DFT/HSE06-D3 band gaps.

Table S10*:* Calculated deviation of band gap (ΔE_g) between DFT/HSE06 and DFT/HSE06-D3 calculations of $CsPbX_3$ 2D films.

system	d / nm	ΔE_g / eV
$PbCl_2$-(001) $CsPbCl_3$	0.5	0.08
CsCl-(001) $CsPbCl_3$	0.5	0.07
Cl-(110) $CsPbCl_3$	0.7	0.05
Cs-(110) $CsPbCl_3$	0.7	0.05
PbCl-(110) $CsPbCl_3$	0.8	0.04
$PbBr_2$-(001) $CsPbBr_3$	0.5	0.06
CsBr-(001) $CsPbBr_3$	0.6	0.10
Br-(110) $CsPbBr_3$	0.7	0.03
Cs-(110) $CsPbBr_3$	0.7	0.10

PbBr-(110) $CsPbBr_3$	0.8	0.06
PbI_2-(001) $CsPbI_3$	0.6	0.02
CsI-(001) $CsPbI_3$	0.6	0.10
I-(110) $CsPbI_3$	0.8	0.01
Cs-(110) $CsPbI_3$	0.7	0.10
PbI-(110) $CsPbI_3$	0.9	0.06

References

1 L. A. Cipriano, G. Di Liberto, S. Tosoni and G. Pacchioni, Quantum confinement in group III–V semiconductor 2D nanostructures, *Nanoscale*, 2020, **12**, 17494–17501.

2 L. Protesescu, S. Yakunin, M. I. Bodnarchuk, F. Krieg, R. Caputo, C. H. Hendon, R. X. Yang, A. Walsh and M. V. Kovalenko, Nanocrystals of Cesium Lead Halide Perovskites (CsPbX 3 , X = Cl, Br, and I): Novel Optoelectronic Materials Showing Bright Emission with Wide Color Gamut, *Nano Lett.*, 2015, **15**, 3692–3696.

3 M. A. Becker, R. Vaxenburg, G. Nedelcu, P. C. Sercel, A. Shabaev, M. J. Mehl, J. G. Michopoulos, S. G. Lambrakos, N. Bernstein, J. L. Lyons, T. Stöferle, R. F. Mahrt, M. V. Kovalenko, D. J. Norris, G. Rainò and A. L. Efros, Bright triplet excitons in caesium lead halide perovskites, *Nature*, 2018, **553**, 189–193.

4 D. Vilela Oliveira, J. Laun, M. F. Peintinger and T. Bredow, BSSE-correction scheme for consistent gaussian basis sets of double- and triple-zeta valence with polarization quality for solid-state calculations, *J. Comput. Chem.*, 2019, **40**, 2364–2376.

5 T. Das, G. Di Liberto, S. Tosoni and G. Pacchioni, Band Gap of 3D Metal Oxides and Quasi-2D Materials from Hybrid Density Functional Theory: Are Dielectric-Dependent Functionals

Superior?, *J. Chem. Theory Comput.*, 2019, **15**, 6294–6312.

6 J. Heyd and G. E. Scuseria, Efficient hybrid density functional calculations in solids: Assessment of the Heyd–Scuseria–Ernzerhof screened Coulomb hybrid functional, *J. Chem. Phys.*, 2004, **121**, 1187–1192.

7 R. W. R. Wyckoff, *Crystal Structures*, Interscience Publishers, New York, New York, 2nd edn., 1963.

8 D. O. Scanlon, C. W. Dunnill, J. Buckeridge, S. A. Shevlin, A. J. Logsdail, S. M. Woodley, C. R. A. Catlow, M. J. Powell, R. G. Palgrave, I. P. Parkin, G. W. Watson, T. W. Keal, P. Sherwood, A. Walsh and A. A. Sokol, Band alignment of rutile and anatase TiO_2, *Nat. Mater.*, 2013, **12**, 798–801.

9 H. Tang, F. Lévy, H. Berger and P. E. Schmid, Urbach tail of anatase <math display="inline"> <mrow> <msub> <mrow> <mi mathvariant="normal">TiO</mi> </mrow> <mrow> <mn>2</mn> </mrow> </msub> </mrow> </math>, *Phys. Rev. B*, 1995, **52**, 7771–7774.

10 M. Lazzeri, A. Vittadini and A. Selloni, Structure and energetics of stoichiometric <math display="inline"> <mrow> <msub> <mrow> <mi mathvariant="normal">TiO</mi> </mrow> <mrow> <mn>2</mn> </mrow> </msub> </mrow> </math> anatase surfaces, *Phys. Rev. B*, 2001, **63**, 155409.

11 F. Liu, Y. Zhang, C. Ding, T. Toyoda, Y. Ogomi, T. S. Ripolles, S. Hayase, T. Minemoto, K. Yoshino, S. Dai and Q. Shen, Ultrafast Electron Injection from Photoexcited Perovskite CsPbI 3 QDs into TiO 2 Nanoparticles with Injection Efficiency near 99%, *J. Phys. Chem. Lett.*, 2018, **9**, 294–297.

12 Z.-J. Li, E. Hofman, J. Li, A. H. Davis, C.-H. Tung, L.-Z. Wu and W. Zheng, Photoelectrochemically Active and Environmentally Stable CsPbBr 3 /TiO 2 Core/Shell

Nanocrystals, *Adv. Funct. Mater.*, 2018, **28**, 1704288.

13 F. Chen, H. Huang, L. Ye, T. Zhang, Y. Zhang, X. Han and T. Ma, Thickness-Dependent Facet Junction Control of Layered BiOIO 3 Single Crystals for Highly Efficient CO 2 Photoreduction, *Adv. Funct. Mater.*, 2018, **28**, 1804284.

14 J. Yu, J. Low, W. Xiao, P. Zhou and M. Jaroniec, Enhanced photocatalytic CO2-Reduction activity of anatase TiO2 by Coexposed {001} and {101} facets, *J. Am. Chem. Soc.*, 2014, **136**, 8839–8842.

15 G. Di Liberto, S. Tosoni and G. Pacchioni, No Title, *Under Rev. J. Phys. Condens. Matter*.